Interlayer correlated fractional quantum Hall state in the ν = 4/5 bilayer system

Hao Wang

Shenzhen Institute for Quantum Science and Engineering and Department of Physics, Southern University of Science and Technology, Shenzhen 518055, China

Alexander Seidel

Department of Physics, Washington University, St. Louis, Missouri 63130, USA

Kun Yang

Physics Department and National High Magnetic Field Laboratory, Florida State University, Tallahassee, Florida 32310, USA

Fu-Chun Zhang

Kavli Institute for Theoretical Sciences, and CAS Center for Topological Quantum Computation, University of Chinese Academy of Sciences, Beijing 100190, China

We perform exact diagonalization studies for fractional quantum Hall states at filling factor 4/5 in a bilayer system, on a torus with various aspect ratios and angles. We find that in the absence of tunneling, two weakly coupled 2/5 layers undergo a phase transition into an interlayer-correlated regime, which is also Abelian with the fivefold degeneracy on the torus. In the limit of zero layer separation, this phase becomes a singlet in the pseudospin variable describing the layer degree of freedom. By studying the Chern-number matrix, we show that the K matrix describing the interlayer-correlated regime requires a matrix dimension larger than two and this regime is in particular not described by a Halperin state. A detailed analysis of possible 4×4 K matrices having the requisite symmetries and quantum numbers shows that there is only one equivalence class of such matrices. A model wave function representing this universality class is constructed. The role of separate particle number conservation in both layers is discussed, and it is argued that this additional symmetry allows for the further distinction of two different symmetry-protected Abelian phases in the interlayer correlated regime. Interlayer tunneling breaks this symmetry and can drive the system into a single-layer regime when strong enough. A qualitative phase diagram in the tunneling-layer separation parameter space is proposed based on our numerical results.

I. INTRODUCTION

Bilayer quantum Hall systems host extremely rich physics, due to the electron's (additional) internal degree of freedom associated with the layer where it resides, as well as the competition between inter- and intralayer electron-electron interactions. In addition to double quantum well systems, a single wide quantum well can also support a bilayer regime, depending on system parameters. Recent experiments observed a fractional quantum Hall (FQH) state at Landau filling $\nu = 4/5$ in such wide quantum well systems [1]. Obvious candidates include the single-layer $\nu = 4/5$ state which is the particle-hole conjugate of the Laughlin $\nu = 1/5$ state in the single-layer regime, and two weakly coupled $\nu = 2/5$ states (one for each layer) in the bilayer regime, with weak interlayer interaction and correlation. Much more interesting is the bilayer regime in which interlayer interaction strength is comparable to intralayer interaction, and interlayer electron-electron correlation cannot be neglected. In this regime, several theoretical model states have been suggested, some of which may be non-Abelian [2–4]. Motivated by these

experimental and theoretical developments, we perform detailed numerical studies of a clean bilayer quantum Hall system at total Landau filling $\nu = 4/5$, with equal population of the two layers and, in most cases, without interlayer tunneling. The effects of interlayer tunneling will be briefly addressed in Sec. IV.

II. MODEL AND NUMERICAL RESULTS

In our numerical calculations, we consider a bilayer electron system subject to a magnetic field B perpendicular to the two-dimensional plane. We use torus geometry with two-dimensional basis vectors $\mathbf{L_x}$, $\mathbf{L_y}$ spanning the unit cell and having an aspect angle θ between them. Unless otherwise stated, numerical results presented in this paper correspond to $L_x = L_y$ and $\theta = \pi/2$, i.e., square unit cell, although we will also consider several other cell geometries. There is an integer number of magnetic flux quanta $N_\phi = L_x L_y \sin\theta / 2\pi \ell^2$ going through the cell, where the magnetic length $\ell = \sqrt{\hbar c / eB}$ is chosen as the length unit and the energy is in units of $e^2/4\pi\varepsilon\ell$. To reduce the size of the Hilbert space, we carry out our
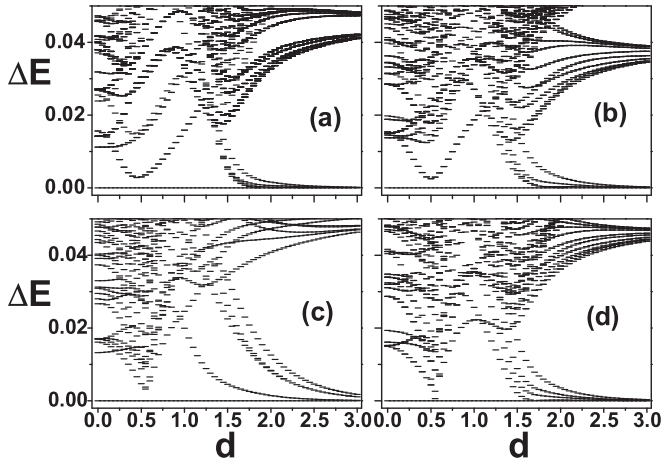
FIG. 1. Low-lying excitation spectra versus layer separation for $\nu = 4/5$ bilayer system with $N_e = 12$ and cell geometries of (a) aspect angle $\theta = 60°$, aspect ratio $r = L_x/L_y = 1.0$ (hexagonal cell); (b) $\theta = 80°$, $r = 1.0$; (c) $\theta = 90°$, $r = 0.8$; (d) $\theta = 90°$, $r = 1.0$ (square cell).

calculation within every pseudomomentum sector $\mathbf{K} = (K_x, K_y)$ [5]. The magnetic field is assumed to be strong enough so electrons can be regarded as spin polarized or spinless [5,6] and confined to the lowest Landau level. The Coulomb interactions are then projected onto the lowest Landau level [5] and can be written in the form

$$ H_c = \frac{1}{N_\phi} \sum_{\mathbf{q} \neq \mathbf{0}, \alpha, \beta} V_{\alpha\beta}(\mathbf{q}) e^{-q^2/2} \sum_{i<j} e^{i\mathbf{q}(\mathbf{R}_{\alpha,i} - \mathbf{R}_{\beta,j})}. \quad (1) $$

Here, $\alpha(\beta) = 1, 2$ are indices referring to the two layers. The momentum $\mathbf{q} = (q_x, q_y)$ takes discrete values suitable for the given unit cell and $\mathbf{R}_{\alpha,i}$ is the guiding center coordinate of the ith electron on layer α. $V_{\alpha,\alpha}(\mathbf{q}) = 1/q$ and $V_{\alpha \neq \beta}(\mathbf{q}) = e^{-qd}/q$ are the Fourier transforms of the intralayer and interlayer Coulomb interactions, respectively, and d is the layer separation. In the present paper, we consider the layers with zero width and performed exact diagonalization to obtain the energy spectrum and eigenstates for a total number of electrons N_e up to 12.

Figure 1 plots excitation energy spectra as functions of layer separation for various unit cell geometries at a system size of $N_e = 12$ with both layers equally occupied and without interlayer tunneling. We start our discussion in the large-d region, where the five lowest energy levels at the pseudomomentum sector (0, 0) form a nearly degenerate group that is clearly separated from higher energy states by a gap. Together with the trivial fivefold center of mass (COM) degeneracy on the torus, this indicates the existence of a 25-fold (nearly degenerate) ground state (GS) manifold. In the $d \to \infty$ limit where two layers completely decouple, we note that these manifold states become exactly degenerate. Each $\nu = 2/5$ layer can be understood as a well-studied 2/5 FQH state, carrying its own fivefold COM degeneracy.

Our numerical calculation shows that the system in the large-d region is actually connected to the decoupled-layer state in the $d \to \infty$ limit, namely a state of two weakly coupled 2/5 FQH layers. A separate calculation has
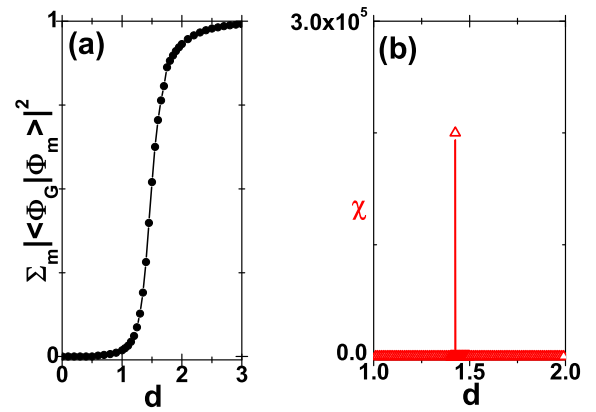

FIG. 2. $N_e = 12$ system at a given GS pseudomomentum sector (0, 0): (a) Sum of squared wave function overlap between ground state and model states versus layer separation. (b) Susceptibility of group fidelity for the five lowest states versus layer separation.

confirmed that, as d grows to infinity, the excitation gap above the GS manifold, $\Delta E_s = E_6 - E_5$, approaches the gap of a $\nu = 2/5$ single layer, and the GS energy of the system approaches twice that of the single layer. The connection can also be exhibited through a comparison of wave functions as shown in Fig. 2(a), where a model state constructed from the single-layer 2/5 FQH states and the ground state Φ_G at pseudomomentum sector (0, 0) of the $N_e = 12$ system are considered. The single-layer 2/5 FQH system of $N_e = 6$ has five degenerate ground states at sectors $(0, 3m)$ for $m = 0, ..., 4$. Then the five basis states Φ_m for the bilayer system at sector (0, 0) can be built as the direct product of these, i.e., $\Phi_m = (0, 3m) \bigotimes (0, k'_m)$ with $k'_m = \mathbf{Mod}(N_\phi - 3m, N_\phi)$. The model state of the bilayer system is considered as a linear combination in this basis. As shown in the plot, the sum of the squared wave function overlaps between Φ_G and these Φ_m continuously evolve to unity in the $d \to \infty$ limit.

The 25-fold degeneracy is of topological origin [10]. As long as the system stays in the weakly coupled-layer phase, it should remain exact in the thermodynamic limit. However, this degeneracy could be lifted by finite-size effect for any $d < \infty$. As shown in Fig. 1, such lifting increases with decreasing d. For nearly all systems at $d = d_{c2} \sim 1.5$, the lifting becomes comparable to the gap and mixing between states below and above the gap starts. Besides of this spectrum feature, the wave function overlap plot in Fig. 2(a) also exhibits a sharp transition around d_{c2}. These observation suggest a quantum phase transition occurring at d_{c2}. To probe the existence of the phase transition at d_{c2}, we performed a fidelity test for the five lowest states ψ_i ($i = 1, .., 5$) at pseudomomentum sector (0, 0). The group fidelity f and its corresponding susceptibility χ are defined as

$$ f = \frac{1}{5} \sum_{i,j=1}^{5} |\langle \psi_i(d - \delta) | \psi_j(d) \rangle|^2, \quad (2) $$

$$ \chi = (1 - f)/\delta^2. \quad (3) $$

The results show a sharp peak around d_{c2}, signifying the quantum phase transition occurring there.

To investigate the nature of the transition at d_{c2}, we turn to the spectrum with d further decreasing. We note that the lowest energy level does not engage in any mixing with other levels, remaining separated by a gap except for $d = d_{c1} \sim 0.5$, where another transition occurs and we will discuss it later. Correspondingly, the GS degeneracy changes to become fivefold below d_{c2}. Thus, the transition at d_{c2} can be interpreted as a transition between the large-d phase of weakly coupled 2/5 layers with 25-fold degenerate ground state, and a topologically different phase with fivefold degenerate ground state at smaller d. Such a transition would also require excited states to become gapless in the thermodynamic limit. A softening of some exited states around $d \sim 1.5$ is clearly seen in the spectra. However, due to finite size effects, the mixing between these softened modes and (some of) the ground states still takes place at finite energy. At large d, the 25-fold ground-state degeneracy signifies a stable topological phase, albeit one with relatively large degeneracy. It is not unexpected that moderate interlayer interactions (at intermediate d) suffice to lower this degeneracy, leading into a different topological phase, with, in this case, minimum COM degeneracy of five. In the following discussion, we will refer to the regions with $d < d_{c2}$ collectively as the interlayer-correlated FQH regime.

As a first step to investigate the interlayer-correlated, small- to intermediate-d region, we carry out numerical studies on the pseudospin excitation in the $d = 0$ limit. In this case, the inter- and intralayer interactions are identical, and the system has a pseudospin SU(2)-symmetry when we identify the layer degree of freedom as a spin-1/2 pseudospin-index in the S_z-basis. Denoting the number of electrons at each layer as $N_\uparrow = N_e/2 + \Delta N$ and $N_\downarrow = N_e/2 - \Delta N$, we then have a total of $S_z = \Delta N$ for the entire system. As a result of the SU(2)-symmetry, eigenstates can be labeled by SU(2) quantum numbers, where states with pseudospin S come in multiplets with $-S \leqslant S_z \leqslant S$. As the numerical results in Fig. 3 show, the GS energy of a balanced-layer system ($\Delta N = 0$ or $S_z = 0$) is found to be the lowest while the GS energy of an imbalanced-layer system increases with ΔN. Furthermore, the GS energy of a $|S_z| = 1$ system exactly matches with the energy of the first excited state of a balanced-layer system. These overlaps in low-energy levels clearly indicate which pseudo-spin sector the excitation of the system belongs to. On the other hand, the GS energy of a $|S_z| = 2$ system is higher. These observations suggest that the $\nu = 4/5$ system at $d = 0$ is a pseudospin-singlet state ($S = 0$), while the lowest-energy excitations form a pseudospin triplet ($S = 1$).

III. TOPOLOGICAL ORDER OF THE INTERLAYER-CORRELATED STATES

We now turn to a more in-depth study of the nature of the topological phase(s) in the interlayer-correlated regime. We first consider a generalized periodic boundary condition with twisted boundary phase angles $0 \leqslant \theta_\eta^\alpha < 2\pi$ along $\eta = x, y$ directions in layer α. After a unitary transformation $\Psi = \exp[-i \sum_\alpha \sum_i ((\theta_x^\alpha/L_x) x_i^\alpha + (\theta_y^\alpha/L_y) y_i^\alpha)]\Phi$, where the summation runs over all electrons of both layers, the resulting many-body wave function Ψ once again satisfies (magnetic) periodic boundary conditions. Many-body topological Chern numbers are then well-defined, and can be given as [7,8]

$$D C_{\alpha,\beta} = \frac{1}{2\pi} \mathrm{Im} \sum_{i=1}^{D} \iint d\theta_x^\alpha d\theta_y^\beta \left\langle \frac{\partial \Psi_i}{\partial \theta_y^\beta} \Big| \frac{\partial \Psi_i}{\partial \theta_x^\alpha} \right\rangle, \quad (4)$$

where the integral is over a phase unit cell of $0 \leqslant \theta_x^\alpha, \theta_y^\beta \leqslant 2\pi$, D is the ground state degeneracy, and i is a label running over a basis of ground states. For the bilayer system with $\alpha(\beta) = 1, 2$, we thus have a 2×2 Chern number matrix (CNM) [8]. The off-diagonal matrix elements $C_{1,2} = C_{2,1}$ are relevant to the boundary-phase-averaged drag Hall conductance. Applying common (opposite) boundary phase on two layers, one can also get the boundary-phase-averaged charge (pseudospin) Hall conductance in units of $e^2/\hbar$ as $C_q = C_{1,1} + C_{2,2} + C_{1,2} + C_{2,1}$ ($C_s = C_{1,1} + C_{2,2} - C_{1,2} - C_{2,1}$). The CNM has been proposed equal to the inverse K matrix for several Halperin hierarchy states in bilayer systems and topological flat bands [9].

We calculated the CNM of the ground states for all the cell sizes, geometries, and ranges of the d parameter considered. For $d < d_{c1}$, the numerical results consistently give a 2×2 matrix,

$$C_1 = \begin{pmatrix} -4/5 & 6/5 \\ 6/5 & -4/5 \end{pmatrix}, \quad (5)$$

whereas for $d_{c1} < d \lesssim d_{c2}$, the numerical results consistently give

$$C_2 = \begin{pmatrix} 6/5 & -4/5 \\ -4/5 & 6/5 \end{pmatrix}. \quad (6)$$

These two regions are separated by a clear gap-closing feature in the spectrum at $d_{c1} \approx 0.5$, where, even at finite system size, the gap closes exactly for some boundary conditions, making the change of CNM possible. Since this transition does not involve a change in ground-state degeneracy, we suspect that it is a symmetry-protected topological phase transition related to the separate conservation of particle number in each layer, a point we will further elaborate on later. For $d \gtrsim d_{c2}$, the lowest five energy states undergo mixing with 20 other states, and the assumption $D = 5$ in Eq. (4) does not lead to consistent results. However, working with the 25 lowest energy states (setting $D = 25$), at sufficiently large d one recovers a CNM

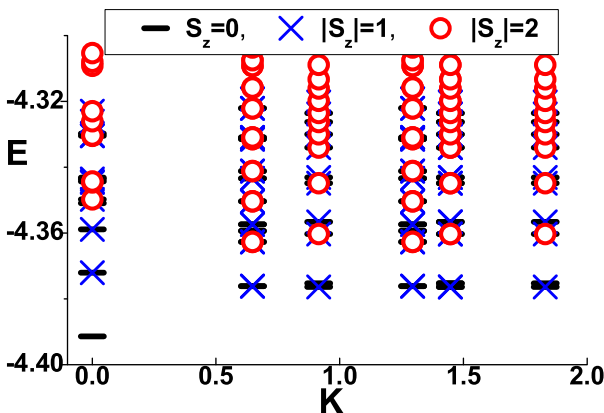

FIG. 3. Comparison of low-lying energy spectra at different total pseudospins $|S_z| = 0, 1, 2$ for $N_e = 12$ system with $d = 0$.

C_3 with diagonal elements equal to 2/5 and zero off-diagonal elements, as expected for two separated 2/5-filling system. Results for $N_e = 8$ particles are very similar, except with smaller intermediate region and earlier onset of the large-d region, which we attribute to finite size effects.

We note that for the large-d system with two separate layers at 2/5-filling, the inverse of the matrix C_3 does not correspond to a proper 2×2 K matrix. This system is actually described by the 4×4 K matrix:

$$K = \begin{pmatrix} 3 & 2 & 0 & 0 \\ 2 & 3 & 0 & 0 \\ 0 & 0 & 3 & 2 \\ 0 & 0 & 2 & 3 \end{pmatrix}. \tag{7}$$

Similarly, the inverses of both matrices C_1, C_2 do not lead to proper K matrices, either. This suggests that the interlayer-correlated regime is *not* described by a Halperin state. Nevertheless, our numerical findings, in particular the fivefold (minimal) torus degeneracy, imply that the interlayer-correlated regime is Abelian. On general grounds, it should then be amenable to a description in terms of symmetric integer K matrix, and a corresponding integer charge vector q. (For a review, see Ref. [10].) The fact that matrices C_1 and C_2 are not obtained as the inverses of proper K matrices suggests that the dimension of the underlying K matrix must be larger than 2, as in the case of C_3 in the large-d limit.

A systematic search for a physically admissible K matrix can be carried out as follows. Since the small-d phase seems to be adiabatically connected to the singlet state at $d = 0$, and since the U(1)-invariance generated by (pseudo-)S_z and (pseudo-)spin flip invariance remain symmetries for any d, the ground state must have $S_z = 0$ and be invariant under spin flip for all d below the phase transition at d_{c_1}. For the K matrix to exhibit this spin flip (or Ising) symmetry, we require it to be of even dimension $2n$ and commute with $\begin{pmatrix} 0 & \mathbb{1} \\ \mathbb{1} & 0 \end{pmatrix}$, where $\mathbb{1} \equiv \mathbb{1}_{n \times n}$ is the $n \times n$-identity matrix. Furthermore, $|\det K|$ must equal the ground-state degeneracy of 5, and $q^t K^{-1} q$ must equal the filling factor of 4/5. Finally, the components of q must be coprime for there to be trivial charge-1, electronlike excitations. There is then always a basis (the "symmetric basis") where all the components of q are 1, and in this basis all diagonal components of K must be odd for the electronlike charge-1 excitations to be fermionic. Indeed, one finds no $n = 1$ (two-dimensional) K matrix that satisfies all these requirements, consistent with our earlier finding that the interlayer-correlated regime is not described by a Halperin state.

For $n = 2$, the most general K matrix thus described has the structure

$$K = \begin{pmatrix} a & b & d & e \\ b & c & e & f \\ d & e & a & b \\ e & f & b & c \end{pmatrix}, \tag{8}$$

with a and c odd, and we take $q = (1, 1, 1, 1)^t$. We carried out a brute force analysis of all such matrices with entries $-13 \leqslant a, \ldots, f \leqslant 13$. There are 447 such matrices

satisfying $|\det K| = 5$ and $q^t K^{-1} q = 4/5$. However, all of these matrices have been found to be congruent via unimodular matrices that leave q invariant. That is, different K, K' in this set are all related via $K' = WKW^t$, where W is an integer matrix with $|\det W| = 1$ and $Wq = q$. K and K' are then physically equivalent [10]. These findings suggest that, up to physical equivalence, there exists only one 4×4 K matrix with the requisite properties, with a suitable representative given by

$$K = \begin{pmatrix} 1 & 2 & 1 & 1 \\ 2 & 1 & 1 & 1 \\ 1 & 1 & 1 & 2 \\ 1 & 1 & 2 & 1 \end{pmatrix}. \tag{9}$$

Any hypothetic K matrix solving our problem while being *inequivalent* to Eq. (9) would need to have entries larger than 13 in the symmetric basis. Thus, Eq. (9) can certainly be viewed as the simplest solution, suggesting that it is, at the very least, the most robust.

Note that Eq. (9) satisfies $\det K = +5$, with two positive and two negative eigenvalues, signifying two copropagating and two counterpropagating bosonic edge modes. These are direct consequences of the bulk topological order encoded in the K matrix, which can be revealed by inspecting edge excitation spectrum when studying disk geometry, or the entanglement spectrum of the ground state itself.

It is prudent to ask what the relation is between the K matrix of Eq. (9) here and the Chern-number matrices discussed early. As mentioned, one of the defining features of Eq. (9) is the relation $q^t K^{-1} q = 4/5$, which defines the filling factor, and, at the same time, the Hall conductance. As such, it is the sum of all matrix elements of the CNM. One may identify $q_1 = (1, 1, 0, 0)^t$ as the part of the charge vector associated to the upper layer, and $q_2 = (0, 0, 1, 1)^t$ the part of q associated to the lower layer, such that $q = q_1 + q_2$. We thus expect the CNM to be given by $C_{i,j} = q_i^t K^{-1} q_j$. Note that for Halperin states, $q_1 = (1, 0)^t$, $q_2 = (0, 1)^t$, which indeed reduces to CNM $= K^{-1}$. With this, the K matrix of Eq. (9) gives matrix C_2 of Eq. (6), corresponding to the region $d_{c_1} < d < d_{c_2}$. But it is inconsistent with the matrix C_1 of Eq. (5) that we found for $d < d_{c_1}$. As already mentioned at the level of the K-matrix description, all K matrices satisfying the constraints described here are equivalent in the topological sense [10] (congruence via unimodular matrices), but not all of these matrices yield the same CNM via the above prescription. This may not be surprising, as the CNM is only well-defined in the presence of an additional U(1)-symmetry, and it is well appreciated that symmetries may *enrich* [11] topological orders, i.e., they may lead to distinctions between phases that are otherwise topologically identical. Indeed, the equivalence class of K matrices defined here does have representatives leading to the CNM C_1 of Eq. (5), the simplest being

$$K' = \begin{pmatrix} 1 & 1 & 1 & 2 \\ 1 & 1 & 2 & 1 \\ 1 & 2 & 1 & 1 \\ 2 & 1 & 1 & 1 \end{pmatrix}. \tag{10}$$

Indeed, Eqs. (9) and (10) are congruent via the unimodular matrix:

$$W = \begin{pmatrix} 1 & 0 & 0 & 0 \\ 0 & 0 & 1 & 0 \\ 0 & 0 & 0 & 1 \\ 0 & 1 & 0 & 0 \end{pmatrix}. \tag{11}$$

In particular, they describe the same edge physics, as well as bulk topological properties in terms of quasiparticle content and statistics.

Finally, we intend to provide in particular the K matrix of Eq. (9) with a simple wave-function interpretation: The diagonal blocks represent, in each layer, a particle-hole conjugate of the Laughlin-1/3 state, $\psi_{2/3}$. The layers are then coupled through a Jastrow-factor $\prod_{1 \leqslant i, j \leqslant N}(z_i - w_j)$ (off-diagonal block), where the z_j (w_j) are the complex coordinates of the upper (lower) layer, thus

$$\psi(z_1, \dots, z_N, w_1, \dots, w_N)$$
$$= \prod_{1 \leqslant i, j \leqslant N} (z_i - w_j) \; \psi_{2/3}(z_1, \dots, z_N)$$
$$\times \psi_{2/3}(w_1, \dots, w_N). \tag{12}$$

We note that a similar wave-function form was also proposed by composite fermion theory [2].

It is worth recalling that the K matrix and charge vector q, by themselves, do not specify the topological shift [12] $\mathcal{S}$ of the state, which is another important piece of the topological data and is defined in $N_\Phi = \nu^{-1} N_e - \mathcal{S}$ with N_Φ the number of flux quanta in spherical geometry. However, the variational wave-function interpretation of Eq. (12) does imply a definite topological shift as follows: One may convince oneself that the factor $\prod_{1 \leqslant i, j \leqslant N}(z_i - w_j)$, applied to any (pseudo-)$S_z = 0$ state, does not affect the topological shift. The topological shift of Eq. (12) must therefore be the same as that of the 2/3 state, which is $\mathcal{S} = 0$. The shift $\mathcal{S}$ only requires rotational invariance in order to be well-defined, but not the separate conservation laws that lead to the distinction of the phases $d < d_{c_1}$ and $d_{c_1} < d < d_{c_2}$. Hence, one may expect the entire interlayer-correlated regime $d < d_{c_2}$ to have the same shift. Thus, to the extent that the wave function of Eq. (12) is the correct description of the intermediate phase $d_{c_1} < d < d_{c_2}$, we expect this shift to be zero in all of the interlayer-correlated regime. A direct verification of this prediction on the sphere, as well as predictions on the edge and entanglement spectra, will provide further support to the topological order we have discussed here. We will leave these considerations for future work.

IV. EFFECTS OF INTERLAYER TUNNELING

We emphasize that well-defined CNMs of C_1 and C_2, separating two distinct regions, can be obtained only in the presence of separately conserved charges in the upper and lower layer, respectively. Under these circumstances, any change in CNM necessarily results in distinct regions separated by a critical point, as happens in the present case, where the CNM changes from C_2 to C_1 at d_{c_1}. On the other hand, if these separate conservation laws are violated via nonzero interlayer tunneling, one would expect that the region
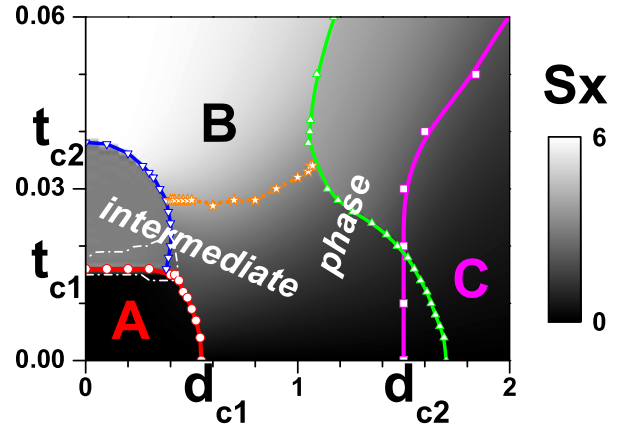

FIG. 4. Magnetization plot for the expectation value of total pseudospin S_x at pseudomomentum sector $(0, 0)$ of $N_e = 12$ system. The phase regions of A, B, C, intermediate phase, and their boundaries are described in the main text.

$d_{c_1} < d < d_{c_2}$ may be adiabatically connected to the region $d < d_{c_1}$ without gap closing. Shedding light on questions such as this, and to further explore the physics of a bilayer system at filling factor 4/5, motivates us to explore an extended phase diagram including interlayer tunneling terms. Thus, we study the following model Hamiltonian with interlayer tunneling parameter t:

$$H' = H_c - t \, S_x + d \, S_z^2 / N_\phi, \tag{13}$$

where the total pseudospin $S_x = \sum_{i, \alpha \neq \beta} a_{i,\alpha}^\dagger a_{i,\beta}/2$ with the creation (annihilation) operator $a_{i,\alpha}^\dagger$ ($a_{i,\alpha}$) for the ith lowest Landau-level orbital in the α layer, and the last term is induced by an imbalance of the electron number in the two layers with total pseudospin S_z [13]. This model will allow us to investigate the phase evolution of the system under the influence of both the layer separation and interlayer tunneling, thus offering a more comprehensive understanding. Through our numerical calculation, we note that the system GS is mostly located at the pseudomomentum sector $(0, 0)$ except for a small parameter region enclosed by the white dashed line in the diagram of Fig. 4. We interpret this to be a spin-density-wave regime, which we argue removable via a perturbation on the Coulomb interaction, e.g., due to layer thickness. Therefore, in the following discussion, we will focus on the ground state within the $(0, 0)$ sector.

With the expectation value of total pseudospin S_x at sector $(0, 0)$ depicted as a background grayscale, we have tentatively plotted an extended $t - d$ phase diagram in Fig. 4 for the $N_e = 12$ system with a square unit cell. The phase diagram of the $N_e = 8$ system with a hexagonal cell has qualitatively similar features. The red/blue/green boundary lines in the diagram have been determined as locations of a level crossing involving the GS in the $(0, 0)$ sector. As is clearly seen from the background grayscale, these crossings are concomitant with jumps in the S_x-expectation value. *Therefore, these lines must be interpreted as lines of first-order phase transitions.* Details regarding the discontinuity of S_x in the $(0, 0)$ sector are shown in Fig. 5.
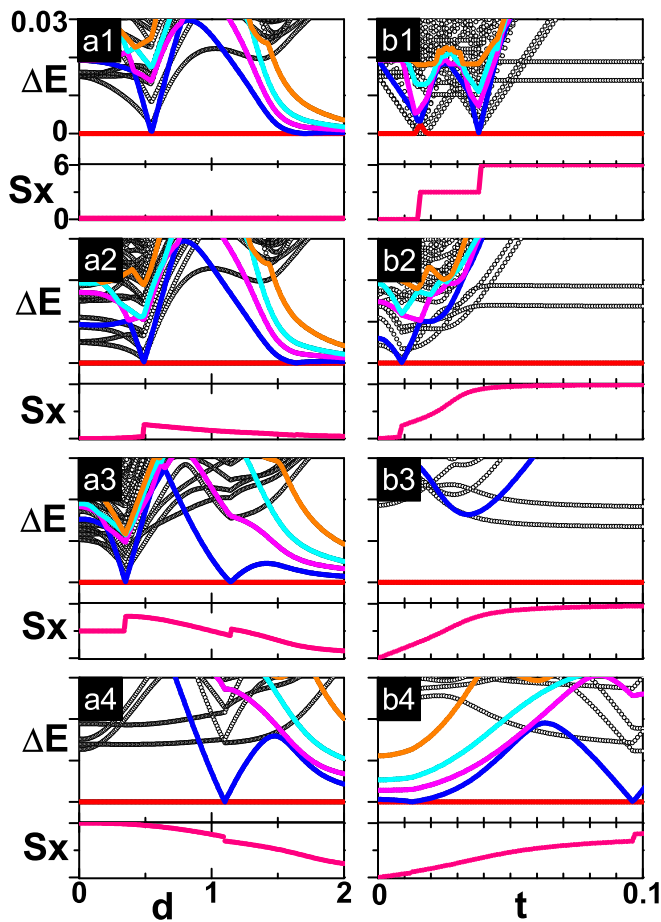
FIG. 5. Low-lying excitation spectrum and expectation value of S_x at pseudomomentum sector (0, 0) for $N_e = 12$ system. Five lowest energy levels at sector (0, 0) are represented by colored curves in the spectra. Plots of (a1)–(a4) stand for system at selected interlayer tunneling parameters $t = 0, 0.01, 0.03, 0.05$; (b1)–(b4) for system at selected layer separations $d = 0, 0.5, 0.8, 1.6$.

We first turn to the system with small interlayer tunneling $t \leqslant t_{c1} \approx 0.015$. As shown in Fig. 5(a2), spectral features are very similar to those previously discussed for $t = 0$, with two phase transitions as d increases. Furthermore, we note that the system within the small t /small d corner, which we termed the A phase, is adiabatically connected to the pseudospin singlet state at $t = 0, d = 0$, with its $S_x \approx 0$. This phase *continues* to be separated via a gap closing from an intermediate regime above the $d_{c_1} < d < d_{c_2}$ line. This is at first surprising, since, as we said initially, absent a well-defined S_z-quantum number (charge conservation in each layer), one would not expect these two regimes to be fundamentally distinct. However, since we have strong evidence that the red phase boundary is first order, there is no contradiction to the notion that these regions can be adiabatically connected in a larger Hamiltonian-space than presently considered. Moreover, the critical point at d_{c_1}, at which the CNM changes along the d axis, serves as the natural second-order terminal point for this line of first-order phase transitions.

We now turn to large layer separation d. Physically, even with moderate finite interlayer tunneling, the bilayer system in the limit $d \to \infty$ will enter the phase represented by two

decoupled 2/5 layers, which we denoted as C phase in the diagram. The (purple) boundary between this layer-decoupled zone and the layer-correlated zone in Fig. 4 is determined by scanning for the onset of a well-defined gap between the lowest five energy levels and the remainder in the spectrum. It can also be determined by the forming signal of the 25-fold degeneracy in wave-function overlap and/or by the group fidelity as we discussed in Sec. II. Based on numerical data, there exists another (green) boundary in the diagram, determined by the GS level crossing and/or S_x-discontinuity. However, we note that the relative position between green and purple boundaries varies for $N_e = 8$ system; the S_x discontinuity at the bottom part of the green boundary is small as t decreases and vanishes at $t = 0$ as shown in Figs. 5(a1), 5(a2), and 5(b4). Also, as shown in Figs. 5(a1)–5(a4), in the large d region, the two crossing levels join the group of the five degenerate ground states [within the (0, 0) sector], which are completely degenerate in the thermodynamic limit. These observations lead us to argue that the separate green and purple boundaries are due to finite-size effects and that these boundary lines would merge into a single boundary, at least below a certain t value, in the thermodynamic limit.

Finally, we look at the limit of large t. For finite d and in the limit $t \to \infty$, the bilayer system effectively becomes a single-layer system as single-particle orbitals must align with the effective field in the x direction. We termed this phase the B phase. The transition from a two-layer system to a one-layer system can be exemplified in the $d = 0$ case, where the symmetry is larger; in particular, the S_x symmetry remains intact. At $t \leqslant t_{c1}$, the system stays as a pseudospin singlet with $S_x = 0$. Further increasing t, the system jumps to a finite S_x and undergoes a sequence of GS level crossing within the (0, 0) sector, ending with an S_x-saturated phase at $t = t_{c2} \approx 0.038$, in which $S_x = N_e/2$ and the system enters the single-layer regime described by

$$K = \begin{pmatrix} 1 & 0 \\ 0 & -5 \end{pmatrix}, \qquad (14)$$
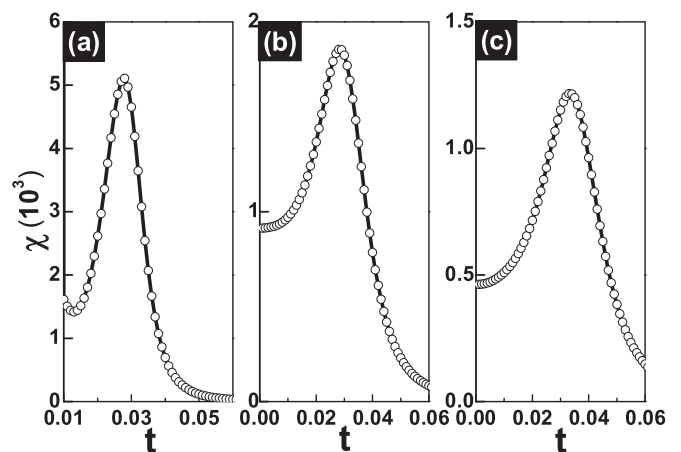

FIG. 6. Ground-state susceptibility at pseudomomentum sector (0, 0) of $N_e = 12$ system with selected layer separations: $d =$ (a) 0.5, (b) 0.8, (c) 1.05.
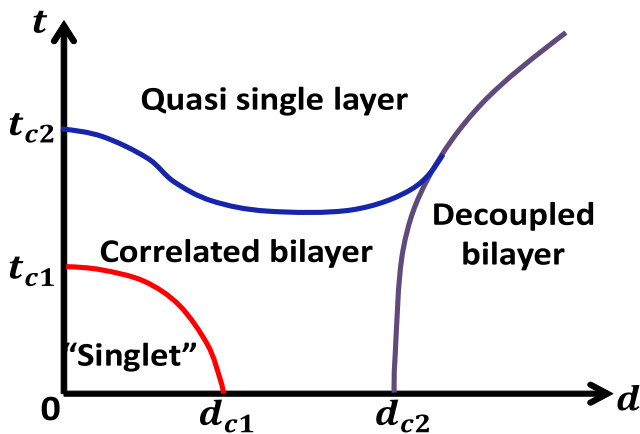
FIG. 7. Proposed $t - d$ phase diagram for the $\nu = 4/5$ bilayer system.

corresponding to the particle-hole conjugate of Laughlin state at $\nu = 1/5$. Although the discontinuity in S_x and/or level crossing in the spectrum are notable in both small-d and large-d regions, as shown by the blue and green lines in Fig. 4, respectively, we note there is no such signal when we increase t in the intermediate-d region as shown in Figs. 5(b2) and 5(b3). However, even along cuts in t with d in this region, we must expect a purely topological phase transition, without change in ground state degeneracy, as we attribute a different K matrix to the $d_{c1} < d < d_{c2}$ interval on the d axis (Sec. III). We have tried to determine the associated phase boundary in this intermediate region (the orange curve in Fig. 4) using GS fidelity. As shown in Fig. 6, when we scan the GS fidelity/susceptibility at a given d, there is a minimum/maximum signal, which we take to be the transition point. This orange boundary merges with the upper parts of the blue boundary and green boundary at its two ends, separating the one-layer phase with $S_x \approx N_e/2$ from the bilayer phase(s).

In the end, we would like to summarize our findings in a schematic $t - d$ phase diagram, Fig. 7, for the $\nu = 4/5$ bilayer system as described by the model Hamiltonian Eq. (13): The system remains a pseudospin-singlet in the small-t/small-d region, becomes a decoupled two 2/5-layer system at large d, and a quasi-single-layer at large t, with a correlated bilayer of fivefold GS degeneracy in the intermediate region.

V. CONCLUSION

We have presented detailed exact diagonalization studies on various toroidal geometries for bilayer FQH states at filling fraction 4/5, with up to $N_e = 12$ particles. We found that for small enough layer separation d, the regime of two weakly coupled 2/5 layers undergoes a phase transition into another Abelian regime, characterized by fivefold (minimal) ground-state degeneracy. The state at zero layer separation has been shown to be a pseudo-spin singlet. We have discussed possible K-matrix descriptions for the Abelian regime with small- to intermediate-d, ruling out all 2×2 K matrices by analyzing the Chern-number matrix in this regime. In the absence of additional conservation laws, we find only one equivalence class of 4×4 matrices with the proper quantum numbers. A model wave function representing this class has been constructed, consisting of two 2/3-states coupled by an interlayer Jastrow-factor. In the presence of separate particle number conservation in each layer, our study suggests the existence of two separate symmetry-protected Abelian phases with identical topological quantum numbers, in particular, identical ground-state degeneracy, but different Chern-number matrix. We have further studied the fate of these phases in the presence of finite interlayertunneling, finding in particular that all phase boundaries survive finite tunneling, but in part become first order. We are hopeful that these findings will stimulate further investigation of this rich and interesting regime in both theory and experiment.

[1] Y. Liu, D. Kamburov, S. Hasdemir, M. Shayegan, L. N. Pfeiffer, K. W. West, and K. W. Baldwin, Phys. Rev. Lett. **113**, 246803 (2014).

[2] V. W. Scarola and J. K. Jain, Phys. Rev. B **64**, 085313 (2001).

[3] M. Barkeshli and X.-G. Wen, Phys. Rev. B **82**, 233301 (2010).

[4] A. C. Balram, C. Toke, A. Wojs, and J. K. Jain, Phys. Rev. B **91**, 045109 (2015).

[5] E. H. Rezayi and F. D. M. Haldane, Phys. Rev. Lett. **84**, 4685 (2000).

[6] R. H. Morf, Phys. Rev. Lett. **80**, 1505 (1998).

[7] D. J. Thouless, M. Kohmoto, M. P. Nightingale, and M. den Nijs, Phys. Rev. Lett. **49**, 405 (1982).

[8] D. N. Sheng, L. Balents, and Z. Wang, Phys. Rev. Lett. **91**, 116802 (2003).

[9] K. Yang, Phys. Rev. B **58**, R4246(R) (1998); Z. Zhu, L. Fu, and D. N. Sheng, Phys. Rev. Lett. **119**, 177601 (2017); T.-S. Zeng, W. Zhu, and D. N. Sheng, Phys. Rev. B **95**, 125134 (2017); **97**, 035151 (2018).

[10] X.-G. Wen, Adv. Phys. **44**, 405 (1995).

[11] X.-G. Wen, Phys. Rev. B **65**, 165113 (2002).

[12] X.-G. Wen and A. Zee, Phys. Rev. Lett. **69**, 953 (1992).

[13] A. H. MacDonald, P. M. Platzman, and G. S. Boebinger, Phys. Rev. Lett. **65**, 775 (1990).